

Supplementary Material

Elucidating Ultrafast Multiphasic Dynamics in the Photoisomerization of Cyanobacteriochrome

Dihao Wang[†], Xiankun Li[†], Lijuan Wang[†], Xiaojing Yang^{*,§} and Dongping Zhong^{*,†}

[†]Department of Physics, Department of Chemistry and Biochemistry, Programs of Biophysics, Chemical Physics, and Biochemistry, The Ohio State University, Columbus, OH 43210, United States

[§]Department of Chemistry, University of Illinois at Chicago, Chicago, IL 60607, United States

Corresponding authors,

E-mail: zhong.28@osu.edu and xiaojing@uic.edu

MATERIALS AND METHODS

Protein Preparation. The tandem sensor domains of WT and three mutants of the cyanobacterium PPHK were overexpressed in *Escherichia coli* BL21 (DE3). The protein expression and purification followed procedures reported previously¹. The steady-state fluorescence emission was measured using a SPEX FluoroMax-3 spectrometer with sample concentration at 5-10 μ M. For the femtosecond-resolved experiments, the PPHK samples were prepared in a 50 mM NaCl and 20 mM Tris buffer (pH 8) with a sample concentration of 50-200 μ M. During the experiment, the samples were under constant illumination of a 530-nm peak output LED (Thorlabs) for a consistent Pr/Pg state ratio and signal level.

Femtosecond Methods. Femtosecond-resolved measurements were taken using the fluorescence upconversion and transient absorption methods. The experimental layout has been described previously². Briefly, for the fluorescence upconversion experiments, the pump pulse was set at 635 nm with the energy attenuated to \sim 100 nJ before it was focused into the sample cell. The fluorescence emission signals were gated by another 800-nm laser beam in a 0.5 mm thick β -barium borate crystal (BBO, type I). For the transient absorption experiments, the probe pulses at the desired wavelengths between 350 and 680 nm were generated via optical parametric amplifiers (TOPAS, Spectra-Physics). The instrument responses are 400 fs and 120-200 fs for fluorescence and transient absorption detection, respectively. All experiments were conducted at the magic angle (54.7°). To prevent heating and photobleaching, the sample was kept in stirring quartz cells with a 1- or 5-mm thickness during laser irradiation. The femtosecond-resolved data were fitting by multiple exponential decays. The transients were fit with multiple exponential decays or rises to deduce the time constants with an error of less than 10% or smaller due to high signal-to-noise ratio.

References

- (1) Shin, H.; Ren, Z.; Zeng, X.; Bandara, S.; Yang, X. Structural Basis of Molecular Logic OR in a Dual-sensor Histidine Kinase. *Proc. Natl. Acad. Sci. U. S. A.* **2019**, *116*, 19973-19982.
- (2) Zhang, L.; Kao, Y.; Qiu, W.; Wang, L.; Zhong, D. Femtosecond Studies of Tryptophan Fluorescence Dynamics in Proteins: Local Solvation and Electronic Quenching. *J. Phys. Chem. B* **2006**, *110*, 18097-18103.

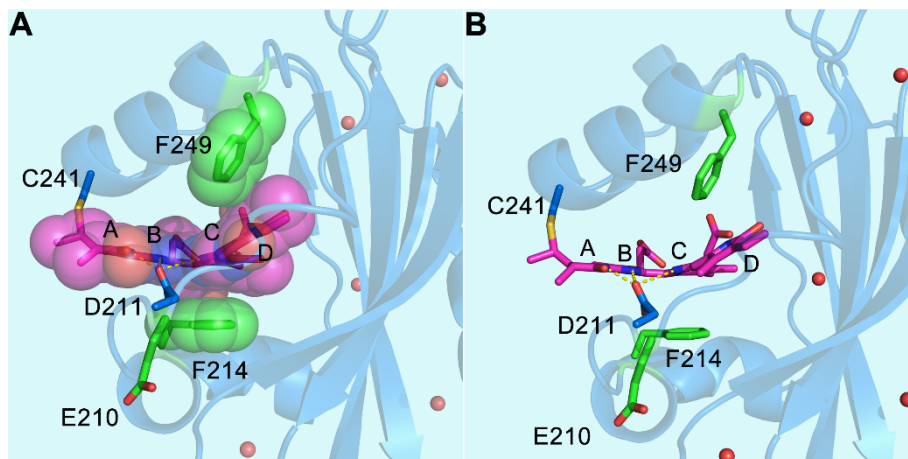


Figure S1. Close-up view of the local chromophore binding pocket with water molecules found in the crystal structure (PDB ID: 6OB8). The A- to C- rings are almost coplanar while the D-ring is relatively tilted in the Pr state. The Phe residues of F214, and F249 (green) are in close contact with the chromophore, as shown in sphere (A) and stick (B) representations.

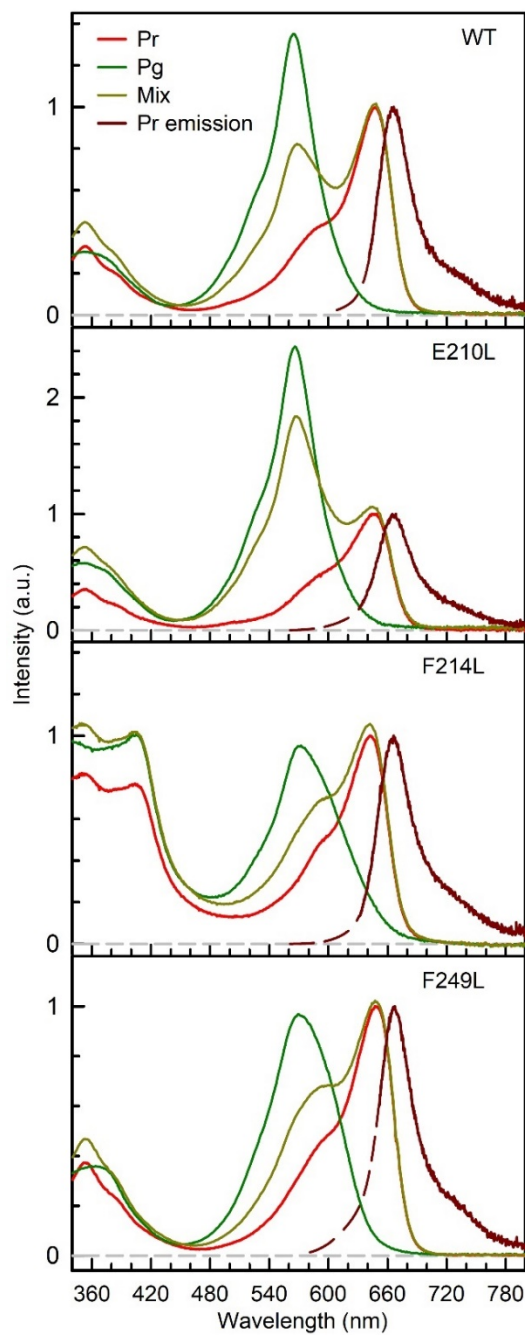


Figure S2. Steady-state absorption spectra of WT and mutants. The mix-state absorption spectra were measured under 530-nm peaked LED light illumination. The pure Pr-state absorption spectra were obtained by conservative subtraction of pure Pg spectra from the mix-state spectra.

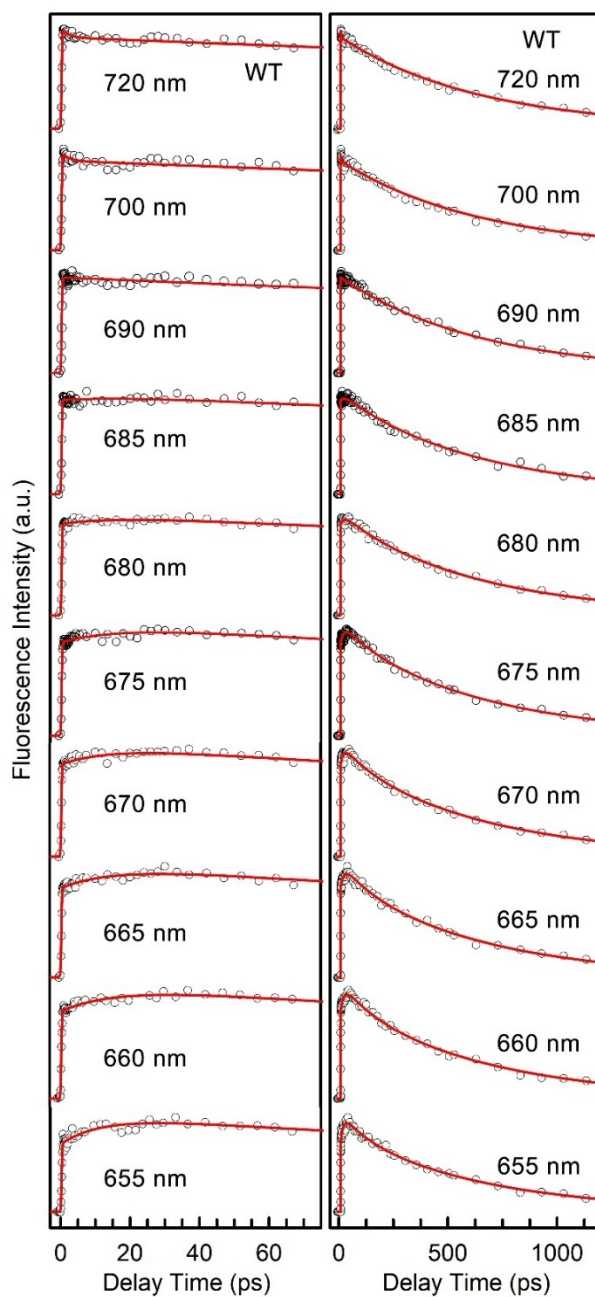


Figure S3. Femtosecond-resolved fluorescence transients of WT PPHK gated from the blue side to the red side of the emission spectra. The symbols are the experimental data and the solid lines are the best exponential fits.

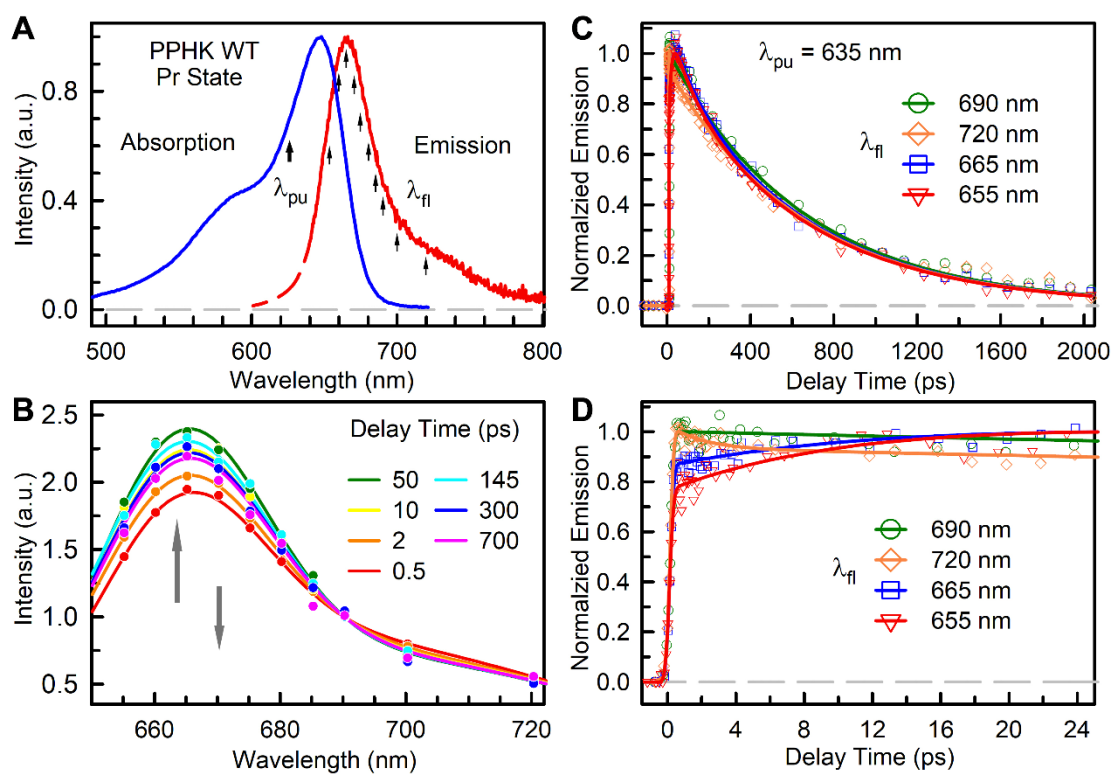


Figure S4. (A) Steady-state spectra of PPHK Pr state. Arrows mark the excitation wavelength and gated fluorescence wavelengths. (B) Constructed FRES of WT PPHK at selected delay times normalized at 690 nm. (C, D) Normalized femtosecond-resolved fluorescence transients gated at several typical wavelengths.

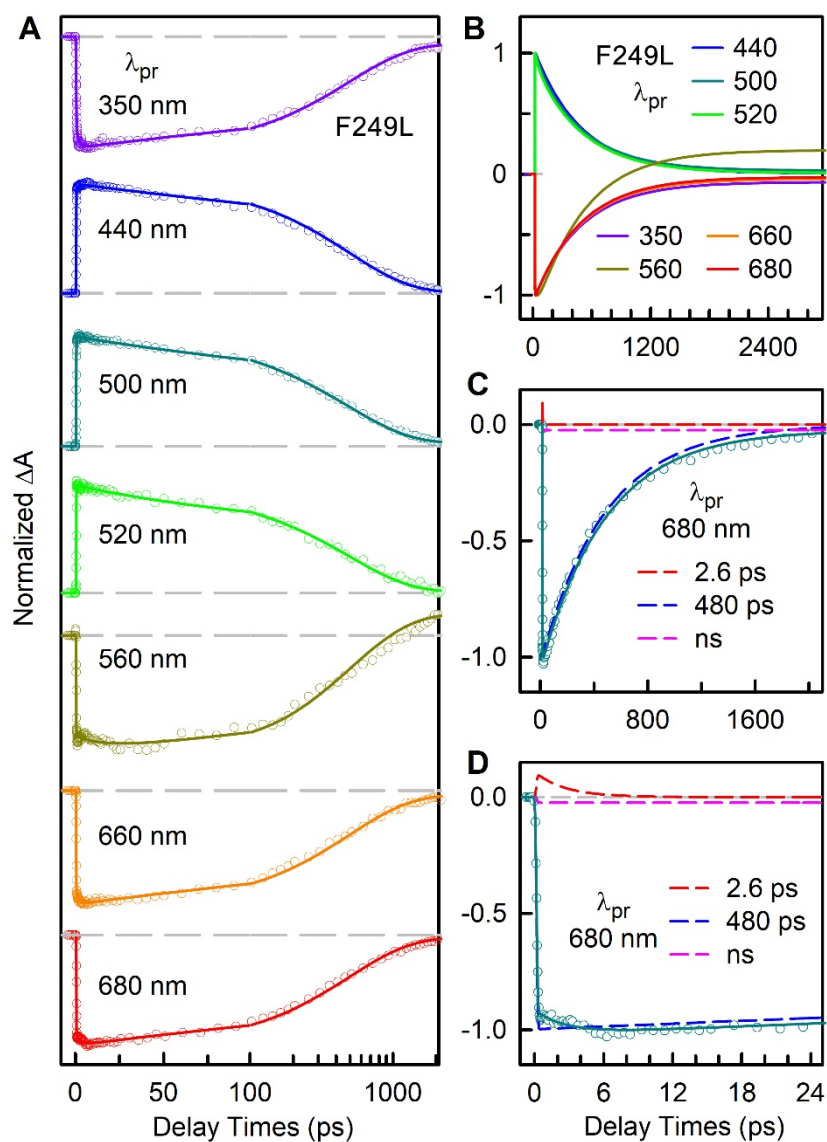


Figure S5. (A) Normalized femtosecond-resolved absorption transients of F249L probed from 350 to 680 nm. (B) Gradual changes of the dynamics with different probe wavelengths. (C) and (D) show the deconvolution of the transients into various dynamic components probed at 680 nm on short and long time scales. All the experimental data are shown in circles and the solid lines are the best exponential fit.

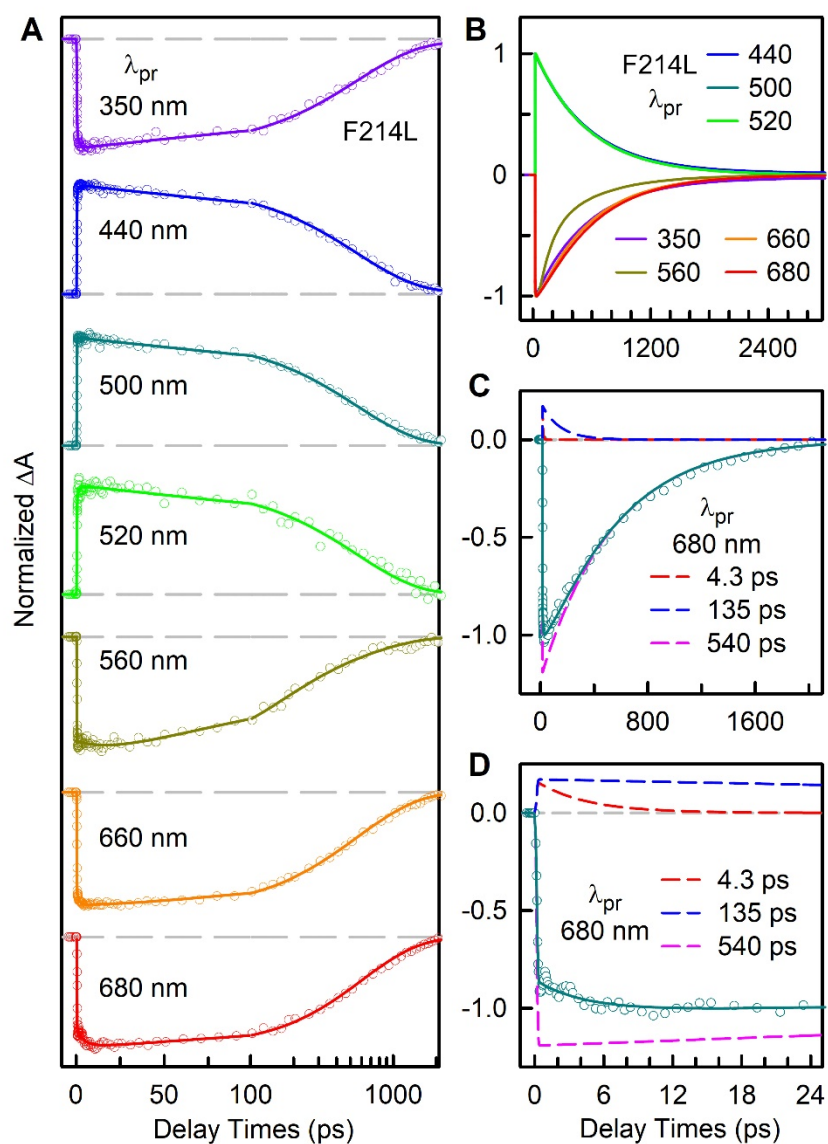


Figure S6. (A) Normalized femtosecond-resolved absorption transients of F214L probed from 350 to 680 nm. (B) Gradual changes of the dynamics with different probe wavelengths. (C) and (D) show the deconvolution of the transients into various dynamic components probed at 680 nm on short and long time scales. All the experimental data are shown in circles and the solid lines are the best exponential fit.

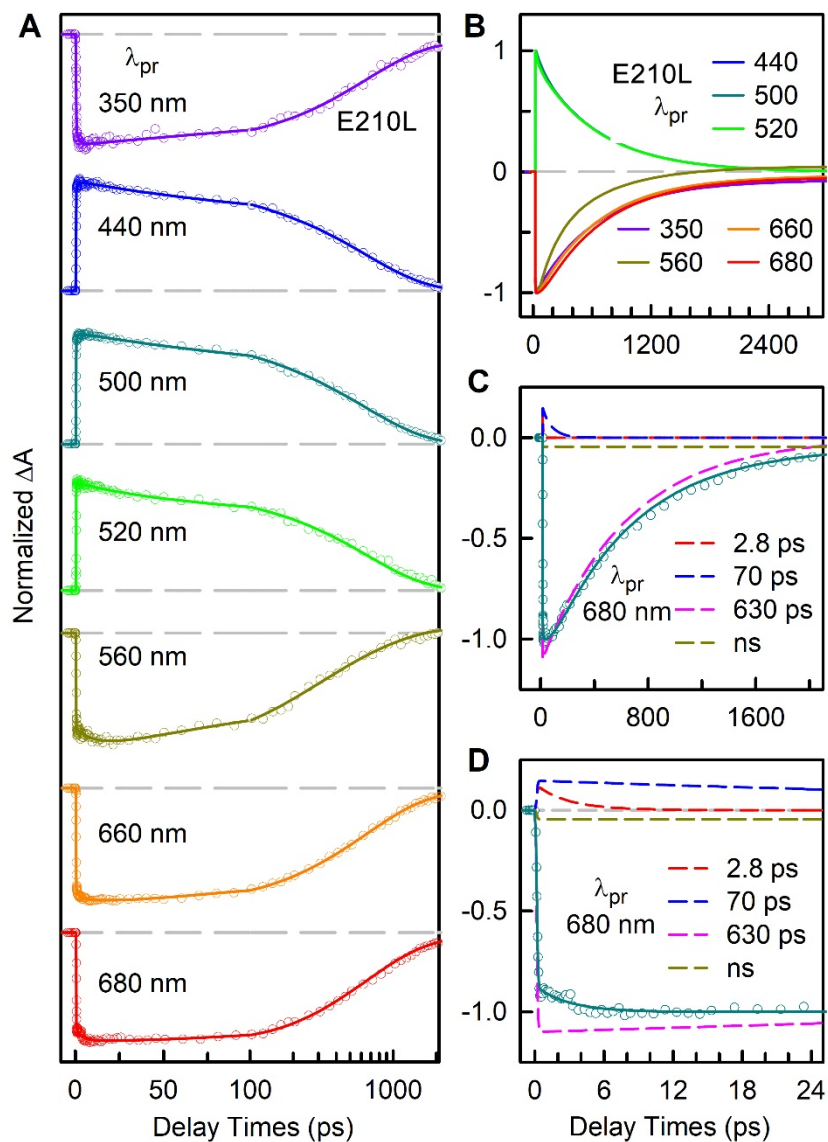


Figure S7. (A) Normalized femtosecond-resolved absorption transients of E210L probed from 350 to 680 nm. (B) Gradual changes of the dynamics with different probe wavelengths. (C) and (D) show the deconvolution of the transients into various dynamic components probed at 680 nm on short and long time scales. All the experimental data are shown in circles and the solid lines are the best exponential fit.

Table S1: WT and mutants steady-state spectral parameters

Steady-State	WT	E210L	F214L	F249L
Absorption (nm)	647	645	642	648
Emission (nm)	665	665	665	666
Mix State (Pg + Pr)	0.38 + 0.62	0.63 + 0.37	0.25 + 0.75	0.27 + 0.73

Table S2: Ultrafast fluorescence dynamics in WT PPHK.^a

	$\lambda_{pu} = 635 \text{ nm}$									
	$\lambda_{fluorescence} \text{ (nm)}$									
	655	660	665	670	675	680	685	690	700	720
τ_1	11.7	16.4	15.1	14.1	16.3	17.5	19.5		1.9	2.0
τ_2	115	112	117	112	114	115	112			
τ_3	640	640	640	640	640	640	640	640	640	640
A_1	-0.31	-0.25	-0.22	-0.19	-0.18	-0.11	-0.07		0.08	0.09
A_2	0.18	0.16	0.15	0.13	0.11	0.06	0.04			
A_3	0.82	0.84	0.85	0.87	0.89	0.94	0.96	1.00	0.92	0.91

^aTime constants are in units of ps. Wavelengths are in units of nm, amplitudes are calculated relative to each other and negative values indicate rise components.

Table S3: Fitting parameters of Pr state WT PPHK transient absorption.

$\lambda_{pr}(\text{nm})$	A_1	A_2	A_3	A_4	τ_1	τ_2	τ_3	τ_4
350	0.21	0.12	-0.93	-0.07	1.2	143	640	ns
440	-0.08	-0.08	1.0		1.2	150	640	
500	-0.09		1.0		2.8		640	
520	-0.02		0.93	0.07	1.9		640	ns
560	0.33	-0.42	-0.58	0.24	16.9	149	640	ns
660	0.13	0.10	-0.96	-0.04	2.7	131	640	ns
680	0.08		-0.95	-0.05	3.8		640	ns

Table S4: Fitting parameters of Pr state F249L PPHK transient absorption.

$\lambda_{pr}(\text{nm})$	A_1	A_2	A_3	A_4	τ_1	τ_2	τ_3	τ_4
350	0.20		-0.94	-0.06	1.5		480	ns
440	-0.05		1.0		1.5		480	
500		0.06	0.91	0.03		86	480	ns
520		0.09	0.91			45	480	
560	0.09	0.11	-1.00	0.14	15	75	480	ns
660	0.11		-0.96	-0.04	1.5		480	ns
680	0.10		-0.98	-0.02	2.6		480	ns

Table S5: Fitting parameters of Pr state F214L PPHK transient absorption.

$\lambda_{pr}(\text{nm})$	A_1	A_2	A_3	A_4	τ_1	τ_2	τ_3	τ_4
350	0.18		-0.98	-0.02	1.2		540	ns
440	-0.05		0.99	0.01	1.2		540	ns
500			1.0				540	
520	-0.13		1.0		1.2		540	
560	0.23	-0.57	-0.43		23.7	123	540	
660	0.11	0.08	-1.0		1.2	49	540	
680	0.13	0.14	-1.0		4.3	135	540	

Table S6: Fitting parameters of Pr state E210L PPHK transient absorption.

$\lambda_{pr}(\text{nm})$	A_1	A_2	A_3	A_4	τ_1	τ_2	τ_3	τ_4
350	0.16		-0.93	-0.07	1.4		630	ns
440	-0.06	0.11	0.89		1.5	66	630	
500	-0.05	0.11	0.89		1.5	88	630	
520		0.10	0.90			34	630	
560	0.20	-0.44	-0.56	0.04	11.4	190	630	ns
660	0.09	0.07	-0.97	-0.03	1.4	21	630	ns
680	0.11	0.13	-0.96	-0.04	2.8	70	630	ns